Biochimica et Biophysica Acta, 945 (1988) 221–245
Elsevier

BBA 74187

Structural properties of a phosphatidylcholine-cholesterol system as studied by small-angle neutron scattering: ripple structure and phase diagram

Kell Mortensen [a], Walter Pfeiffer [b], Erich Sackmann [b] and Wolfgang Knoll [c]

[a] *Physics Department, Risø National Laboratory, Roskilde (Denmark),* [b] *Physics Department E22, Biophysical Group, Technical University Munich, Garching (F.R.G.) and* [c] *Max-Planck Institute für Polymerforschung, Mainz (F.R.G.)*

(Received 5 May 1988)

Key words: Phospholipid bilayer; Cholesterol; Phase diagram; Ripple structure; Fractal structure; Small angle neutron scattering

Small-angle neutron scattering has been used to study structural features of lamellar bilayer membranes of dimyristoylphosphatidylcholine (DMPC) and DMPC mixed with various amount of cholesterol. The studies were recorded at a fixed hydration level of 17% ^2H_2O, i.e. just below saturation. Bragg reflections gives information on the ripple structure and on the bilayer periodicity. The crystalline L_c phase, which was stabilized after long time storage at low temperature, exhibits major small angle scattering when cholesterol is mixed into the membrane. The intermediate $P_{\beta'}$ gel-phase, which is characteristic by the rippled structure, is dramatically stabilized by the introduction of cholesterol. The ripple structure depends significantly both on the cholesterol content and on the temperature. At high temperatures, $T > 15\,^\circ C$, the inverse ripple periodicity varies basically linearly with cholesterol content, and approach zero (i.e. periodicity goes to infinite) at 20 mol% cholesterol, approximately. At lower temperatures the correlation is more complex. The data indicate additional phase boundaries below 2 mol% and at approx. 8 mol%. Secondary rippled structures are observed in the low temperature $L_{\beta'}$-phase for cholesterol content below approx. 8 mol%. The data gives detailed insight into the phosphatidylcholine cholesterol phase diagram, which is discussed on the basis of a simple model in which the cholesterol complexes are fixed to the defect stripes of the rippled structure.

I. Introduction

Biological membranes are bilayers formed by hydrated phospholipids as the basic building unit, and various additives. From a physical point of view, the lipid bilayers are liquid crystals within a smectic phase which depends on lipid composition and temperature as the most important parameters. A very important additive to the plasma membranes is cholesterol, which appear to have astonishing influence on the membrane properties. The study of interaction between phospholipids and cholesterol have therefore recently attracted a lot of interests.

The phase diagram of phospholipid bilayers has been studied by numerous techniques. Most of the work have been concentrated on two of the phase transitions, and the corresponding three phases. These are the two crystalline solid (gel) phases with conformationally ordered acyl chains, denoted $L_{\beta'}$ and $P_{\beta'}$ respectively, and the liquid crystalline phase with conformationally disordered acyl chains, denoted L_α [1]. The transition at T_m between the $P_{\beta'}$ gel-phase and the liquid L_α phase is the so-called main phase transition. At a lower temperature, T_p, the bilayer undergoes a gel-gel

Correspondence: K. Mortensen, Physics Department, Risø National Laboratory, Postboks 49, DK-4000 Roskilde, Denmark.

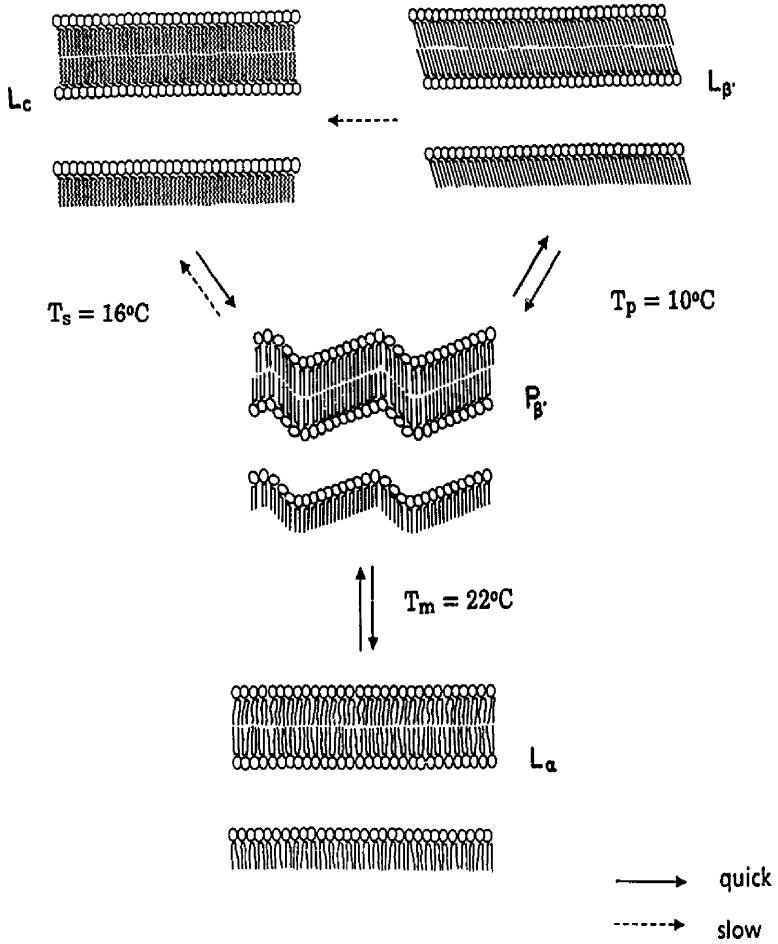

Fig. 1. Schematic illustration of the four phases, L_c, $L_{\beta'}$, $P_{\beta'}$ and L_α, of lamellar amphiphilic layers, as they conventionally are expected to be like. The observed transition temperatures of pure DMPC-d_{54} are included in the diagram. Arrows with solid lines represent quick kinetics involved in the phase transformation (of the order of minutes or less), while the arrows with broken lines represent slow kinetics (of the order of months).

phase transition, which at the present, however, is not understood in detail. Conventionally, the pretransition is associated with the ceases of the characteristic corrugated surface profile, the ripples, which frequently have been observed in the upper $P_{\beta'}$ phase [1–9]. However, both Sackmann et al. [3] and Coleman and McConnel [4] have on the basis of freeze-fracture electron microscopy studies, in addition observed modulated structure in the low temperature $L_{\beta'}$ phase, although the $L_{\beta'}$ undulations might be different from those of the $P_{\beta'}$ phase. The present neutron scattering investigation confirms these results of different kinds of ripples within the $L_{\beta'}$ and $P_{\beta'}$ phases.

The present study strongly suggests that cholesterol tends to decrease the tilt angle of the acyl chain, for eventual to be orthogonal to the bilayer plane within the gel states. The obtained data show moreover marked variation in the ripple structure, which may indicate that the $P_{\beta'}$ phase in reality is composed of different phases, dependent on temperature and cholesterol con-

tent. These features can, though, also be due to changes in the physical parameters dominating the ripple formation.

A third basic phase transition is observed when the material has been at low temperature for a long time. Then the hydrocarbon chains crystallize into a highly ordered phase, called L_c [10]. The kinetics involved in the creation of the L_c phase depends on size of acyl chains and temperature. Typically, the time of L_c formation is of the order of days or months. The L_c to $L_{\beta'}$ or L_c to $P_{\beta'}$ phase transitions (depending on phosphatidylcholine hydrocarbon length) are, on the other hand, quick. In Fig. 1 the four phases and the corresponding phase changes are schematically represented.

In dimyristoylphosphatidylcholine (DMPC), the subtransition temperature is above the pre-transition temperature, $T_s > T_p$ (Fig. 1 and Ref. 10). Details on the experimentally established phases are therefore critically dependent on the thermal history of the sample. We have accordingly performed the series of measurements in well defined, comparable thermal cycles, as described below.

Introducing cholesterol into the phosphatidylcholine bilayer causes remarkable behaviour. At low cholesterol concentrations a slight broadening of the main phase transition has been reported, whereas at higher concentrations the liquid phase of the bilayer is dramatically stabilized [11]. Mabrey et al. found a slight depression of the main transition versus content of cholesterol, whereas Recktenwald and McConnel [13] did not see any change in the transition temperature up to 20 mol%. Knoll et al. [12] have on the basis of neutron scattering studies on liposomes in excess water pointed to lateral phase separation of the gel state leading to an immiscibility gap between 8 and 20 mol% cholesterol, approximately.

The ripple structure and the effect of cholesterol have already been studied by various groups, however, with somewhat contradicting results. Studies based on freeze-fracture electron microscopy [3–8] and X-ray diffraction [1,2] result in ripple periodicity of 120 Å for DMPC. Freeze fracture images of small vesicles, i.e. those with major curvature, show in addition regions of secondary ripples with wavelength of about 260 Å. This long wavelength structure have not been reported in diffraction studies, presumably due to negligible content of the curved regions in the lamellar samples used for diffraction studies. Sackmann et al. [3], Copeland and McConnel [4] and Knoll et al. [8] found in some samples also long wavelength ripple structures at temperatures well below the pretransition temperature. The $P_{\beta'}$ ripple periodicity was by Copeland and McConnel [4] and by Hicks et al. [6] reported to decrease with the content of cholesterol, and above 20 mol%, no rippling was observed. Knoll et al. [8], on the other hand, found no change in periodicity for up to 8 mol% cholesterol, and for $x_c > 0.08$, x_c being the mol% of cholesterol, the observed ripple distance strongly fluctuates.

The present work deals with neutron scattering studies on lamellar structures of perdeuterated dimyristoylphosphatidylcholine (abbreviated DMPC-d_{54} in the following) incorporated with various amount of cholesterol. The hydration (^2H_2O) level is fixed at 17%, i.e. just below saturation. The diffraction data gives direct information on the bilayer periodicity, and in particular information on the ripple structure of $(\text{DMPC-}d_{54})_{1-x_c}$ + $(\text{cholesterol})_{x_c}$ versus content of cholesterol, x_c, and temperature, T.

The ripple structure is clearly seen in the $P_{\beta'}$ phase of the pristine DMPC-d_{54} material, however, as in previously reported scattering experiments [1,2], only one kind of ripples appear in this phase. In the $L_{\beta'}$ phase, on the other hand, a secondary long wavelength ripple structure appears, probably equal to that observed in some freeze-fracture studies [3,4,8]. These features are more clear in the samples of low cholesterol content. In the 2 mol% cholesterol bilayer material there is a distinct overlap in temperatures, where two kind of ripples are present. The 4 mol% material shows also evidence of a secondary ripple at low temperature. In the samples with 8 mol% cholesterol and more, there is no longer any evidence of the pre-transition, and in the 8 and 14 mol% cholesterol materials, the presumably primary ripple structure remains to the lowest temperatures studied ($T = 5\,^\circ\text{C}$). The $x_c = 0.18$ composition did not show any scattering peaks reflecting rippled structure. Still, however, major small angle scattering strongly suggests some kind of fluctuating rippled structure, although they are

too disordered to give rise to Bragg reflections. No sign of ripples are observed for cholesterol content of 24 mol%.

Generally, the introduction of cholesterol causes increasing ripple periodicity. However, as the cholesterol also gives rise to marked temperature dependence of the periodicity, the relationship between periodicity and cholesterol is certainly not trivial.

The scattering data show no evidence of rippled structure in the melted L_α-phase, nor in the crystalline L_c phase. However, major small angle scattering at low temperatures indicates complex texture of the L_c phase, eventually resulting from some kind of cholesterol segregation.

II. Materials and Methods

II.1. Materials and sample preparation

Dimyristoylphosphatidylcholine with perdeuterated fatty acid chains (DMPC-d_{54}) was obtained from Avanti (Birmingham, AL) and cholesterol was obtained from Serva (Heidelberg, F.R.G.). All lipids gave a single spot on thin-layer chromatography and were used without further purification.

For sample preparation, DMCP-d_{54} and cholesterol were dissolved in $CHCl_3$ solvent. The solvent was afterward evaporated under dry nitrogen atmosphere and subsequently further dried in vacuum to remove traces of the $CHCl_3$ solvent. 20% ^2H_2O was then put into the composition, and the sample was sealed and equilibrated in an oven at 50°C for 2 h. This preparation procedure yields a final water content of 17 wt%, (where 'wt' is with regard to the corresponding amount of non-deuterated water, H_2O). The lipid-cholesterol mixtures were finally filled into quartz cells, sealed and tempered at 80°C for 8 h. The final amount of water was determined after the experiments using a Mitsubishi moisture-meter MCI model CA-02 according to the Karl Fischer method.

II.2. Sample treatment

The samples were contained in special made holders with quartz windows. The sample thickness was 0.2 mm and the effective area seen by the neutrons was 6 mm diameter. The holders were one by one situated in a thermostated sample chamber, of which the temperature was controlled to 0.5°C.

The data presented in this paper represent all samples, which have been stored at 5°C for more than a month before the series of measurements were performed. This procedure was done to stabilize the crystalline L_c phase. The sample was then within approx. 15 h heated stepwise to 30°C, which is well in the liquid L_α phase. At each level, scattering measurements were performed. After the heating to 30°C the sample was cooled to 5°C, while measuring, and successively heated a second time to 30°C. Generally, the data obtained during the cooling and during the second heating (marked metastable in the figures below) were equal, while the data of the initial heating (marked stable in the figures) showed different behaviour. Some of the materials were in addition measured shortly after preparation. These scattering data were all in agreement with those of the later annealed (i.e., metastable) specimens, presented below. Some of the samples were moreover studied a second time after storage at 5°C for months. Except for the sample with 4 mol% cholesterol, the data was unchanged relative to that observed previously, including small angle scattering and properties on ripple. These features are in agreement with the slow kinetics involved in the formation of the crystalline L_c phase, and quick kinetics in the annihilation of the L_c phase and in the pre and main phase transitions. Thus, we believe that the initial (stable) scattering curves represent data of the $L_c \rightarrow P_{\beta'} \rightarrow L_\alpha$ phase diagram, and the successive data (metastable) represents the $L_{\beta'} \rightarrow P_{\beta'} \rightarrow L_\alpha$ phase diagram. Some hysteresis was, though, found in the ripple and bilayer structure of pristine DMPC-d_{54}, and the sample with 4 mol% cholesterol showed some hysteresis in small-angle scattering at low temperatures. These features will be discussed below. In the 4 mol% material, the ripple was not observed when the sample was reexamined several months after the first study, thus pointing to some kind of degradation of that sample.

II.3. Small-angle neutron scattering experiments and data evaluation

The neutron scattering experiments were performed using the small-angle neutron scattering

(SANS) camera at the cold source of Risø National Laboratory. The neutron beam was monochromatized using a mechanical velocity selector, with a setup resulting in a resolution of $\Delta\lambda/\lambda = 0.18$. The 2.25 m collimation system had a 6 mm aperture in front of the sample and the entrance aperture after the velocity selector was 14 mm. The distance between sample and detector was 3.00 m. The scattering data were recorded using a 59 cm diameter area-sensitive ^{3}He-proportional counter, and a beam-stop of 4 cm diameter was used to catch the direct beam. The neutron wavelength was $\lambda = 3.5$ Å for studies of the bilayer repetition length. For studies of the ripple structure, $\lambda = 8$ Å, 15 Å and 24 Å were used. The $\lambda = 3.5$ Å neutron spectra were recorded within 10 min, the $\lambda = 8$ Å spectra within 30 min, and the 15 and 24 Å spectra were recorded within 1–2 h.

For the background correction, to be subtracted from the raw data files, we used for the spectra obtained with neutron wavelength of 8 Å or more the raw 30°C spectra of the samples themselves. These L_α-spectra showed no significant structure, except for minor small angle scattering dominated by artificial effects (window etc.), and incoherent scattering of the sample. The pure DMPC-d_{54} lipid showed though some unreproducible scattering at the smallest angles, maybe due to bubbles in the sample. Unfortunately, we therefore had to disregard the scattering data of that material for scattering vectors below $q = 0.011$ Å^{-1}. For the spectra obtained using $\lambda = 3.5$ Å neutrons, a modified version of the 30°C spectra were used, in which the (10)-bilayer Debye-Scherrer ring was eliminated by software. The two-dimensional scattering data were corrected for inhomogeneities in the detector efficiency by using the incoherent scattering from water, and finally they were 'normalized' by multiplication with a constant factor. This normalization-factor makes all spectra obtained to be directly comparable, as one intensity unit (arbitrary unit in the figures) are the same in all data presented below.

All spectra obtained showed circular symmetry of the 2D-data files. After background correction and normalization the two-dimensional data were reduced by radially averaging, thus giving the final intensity (I) versus scattering vector (q) data presented in the Figs. 2–8 and 11–17 shown below.

III. Experimental results

The neutron scattering diffraction pattern shows Bragg reflections which we attribute to (1) the bilayer periodicity and (2) the rippled structure of the lamellar planes. The reflection peaks were fitted to Gaussian form, and the bilayer and the ripple periodicities were obtained using Braggs law, $d = 2\pi/q$. The bilayer reflections, which have wavevector of the order of $q = 0.1$ Å^{-1} is within the limited q range only for data sets obtained at neutron wavelength 3.5 Å^{-1}. The ripple reflection was studied at suitable wavelength, typically 8 or 15 Å.

The data exhibit features which will be discussed in detail for each composition below. In the low temperature L_c phase, major small angle scattering dominates at q values below approx. 0.04 Å^{-1}, though somewhat depending on the sample. Only the phosphatidylcholine bilayer with 24 mol% cholesterol shows no significant small-angle scattering after storage at 5°C.

The Bragg peaks related to the bilayer periodicity exhibit major temperature dependencies, which clearly reflect the transitions between the various phases. This is mainly marked in the bilayers with cholesterol. There they show in addition a dependence on the cholesterol content and give evidence of a phase boundary near 20 mol% cholesterol.

III.A. Bilayer periodicity

In Fig. 2 is shown representative neutron scattering results of DMPC with perdeuterated acyl chains (DMPC-d_{54}) and various content of cholesterol, as obtained at $T \simeq 11$°C and with neutron wavelength 3.5 Å. The diffraction peak corresponding to the bilayer repetition length (the (10)-reflection) dominates the scattering pattern. Also the ripple structure gives rise to reflections in these spectra. For the bilayer system of 14 mol% cholesterol the ripple reflection is only badly resolved in the 3.5 Å spectra, and moreover it is partly covered by the beam stop. In Fig. 2, the $x_c = 0.14$ data of $q < 0.03$ Å^{-1} are therefore those obtained by 8 Å neutrons. No fitting parameters have been used to merge the two sets of data. Significant small angle scattering is observed in the 'stable state'.

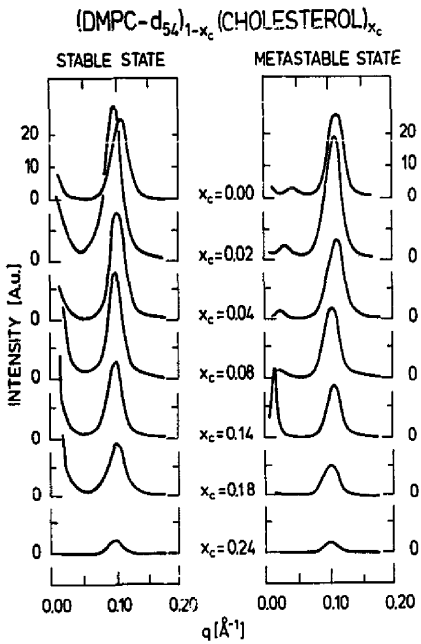

Fig. 2. Neutron scattering results, intensity versus scattering vector q of DMPC-d_{54} with various content of cholesterol as obtained at $T = 1°C$. The data show both the Bragg reflection due to bilayer periodicity and due to ripple structure. The stable state represents initial set of data, following the phase sequence $L_c \rightarrow P_{\beta'} \rightarrow L_\alpha$, whereas the metastable state represents data obtained during cooling from 30 °C, i.e. $L_\alpha \leftrightarrows P_{\beta'} \leftrightarrows L_{\beta'}$.

For all measurements obtained, except that of the pristine DMPC-d_{54}, the spectra of the metastable phases were perfectly reproducible within the time of a temperature cycle from 30 °C to 5 °C to 30 °C (approx. 30 h), i.e., the data obtained during cooling and the successive heating were equal.

III.A.1. DMPC-d_{54}

For the pristine DMPC-d_{54} bilayer sample, the data of the second heating gave marked differences relative to those of the preceding cooling run. The data of the second heating showed results which to a large extent are similar to the initial run, presumably going through the phases $L_c \rightarrow P_{\beta'} \rightarrow L_\alpha$. The bilayer periodicity was exactly equal to that of the initial measurements, and the intensity showed temperature dependence similar to that of the initial data, although the absolute values were slightly smaller after the thermal treatment. These features are more clearly seen in Fig. 3, which show the bilayer periodicity, and the corresponding peak intensity versus temperature for each of the samples examined.

During the second heating of the DMPC-d_{54} sample, the reflection peak showed marked tails at the low-q side (Fig. 2, see also Fig. 5). This tail, which was not seen neither during the initial heating, nor during the cooling of the material, appeared at 6 °C, approximately, and disappeared at roughly 14 °C.

The bilayer periodicity obtained from our neutron scattering studies on the pristine DMPC-d_{54} material are in good agreement with the results on DMPC obtained for 17% hydration [2]. Also the temperature dependence of the bilayer periodicity during the heating of DMPC-d_{54} is very similar to that observed by Janiak et al. [2], who, however, did not include the L_c phase. Mattai et al. [9] have studied other phosphatidylcholine bilayer systems at some discrete temperatures, including the L_c phase, and also found results which qualitatively are equal to those of DMPC-d_{54}.

Knoll et al., who studied DMPC in saturated non-deuterated excess water, H_2O, reported a reduction in the main transition temperature from 23.5 °C to 17.5 °C, when DMPC is substituted with the deuterated analog, DMPC-d_{54} [12]. In the present study, which deals with multi-lamellar structures below water saturation (20%), we find significant higher transition temperatures, namely values which are close to those of DMPC at high H_2O-content. We believe that if the sample was saturated with ^2H_2O excess water, we would find values which are basically identical to those obtained in H_2O. The higher values actually observed are probably due to the water level below saturation. This is known to cause increasing transition temperatures [14]. For the $P_{\beta'} \leftrightarrows L_\alpha$ phase transition, the marked change in lattice parameter reveal a main-transition temperature of $T_m = 22°C$. The $L_c \rightarrow P_{\beta'}$ and the $L_{\beta'} \leftrightarrows P_{\beta'}$ phase changes are less clearly determined from the study of the bilayer repetition length, although modified behaviour are observed both in T dependence of periodicity and in the intensity of the corresponding Bragg peak at $T = 12°C$ (see also the discussion below).

III.A.2. DMPC-d_{54} mixed with cholesterol

The effect on the bilayer periodicity when the DMPC-d_{54} lamellar systems are mixed with cholesterol, is generally an enhanced lattice parameter, however, with a degree and functionality which markedly depends on which state the bilayer system is in. This is seen directly in Fig. 3, for example, but appears even more clearly in Fig. 4a.

In the liquid L_α phase, the bilayer periodicity changes gradually with content of cholesterol. For 0 mol% we find the lattice parameter at 30 °C to be $a = 52$ Å, and at the maximum cholesterol content studied, $x_c = 0.24$, the bilayer periodicity has increased to 58 Å. This increase could be due to stiffening of the fluid chains with increasing cholesterol content.

In the gel states, the dependence on cholesterol is markedly different. The major effect of cholesterol appears already in the low concentration regime: In our study between the pristine material and the material with 2 mol% cholesterol. From 0 to 2 mol% cholesterol, the lattice parameter is markedly enhanced, whereas it only depends slightly on the further cholesterol content. Hui and He [15] found qualitatively similar results studying, presumably, the $L_{\beta'}$, $P_{\beta'}$ and L_α phases of DMPC in H_2O.

The $L_{\beta'}$ to $P_{\beta'}$ pre-transition is in none of the bilayer materials accompanied by significant changes in bilayer periodicity, but perhaps a slight change in the slope of periodicity versus temperature (Fig. 3). At the main transition, on the other hand, both the pristine sample and the materials with small cholesterol content show marked changes in bilayer repetition length. The samples with 2 and 4 mol% cholesterol show modification in the periodicity quite similar to that of the pristine material, whereas further amount of cholesterol cause a reduced change of the lattice parameter. At cholesterol content above 18 mol% there is only minor, if any, changes.

The most dramatic effect is seen in the crystalline, stable L_c phase (Figs. 3 and 4a). It appears from the temperature dependencies shown in Fig. 3, that the characteristics of the sub-phase changes dramatically when small amounts of cholesterol (< 2 mol%) are induced. While the pristine DMPC-d_{54} material only shows a minor change in bilayer repetition length, when going from the crystalline sub-phase to the $P_{\beta'}$ gel-phase, the cholesterol induced bilayers show dramatic changes (Figs. 3 and 4b). For cholesterol content of 2 mol%, the change in the lattice parameter

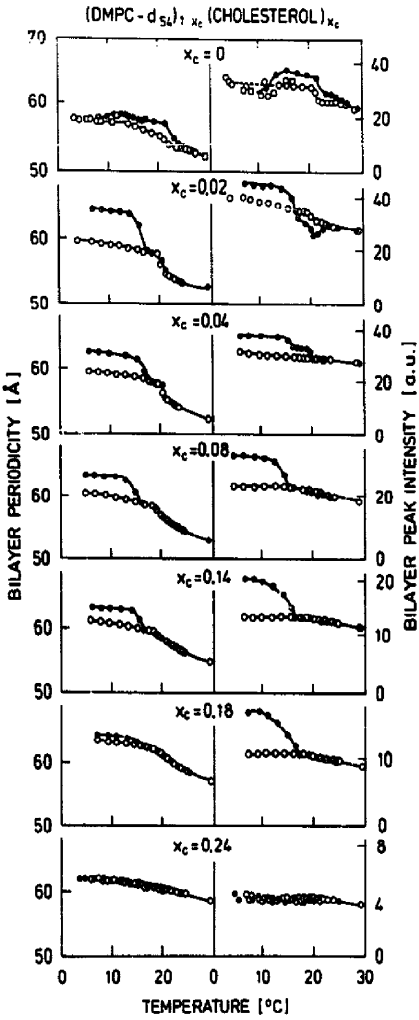

Fig. 3. bilayer periodicity (left column) and peak intensity (right column) of DMPC-d_{54} with various content of cholesterol, as obtained from Gaussian fits to the diffraction data of Figs. 2–8. Note the different scales on the intensity plot. The closed symbols represent data of the stable state, whereas open symbols are those of the metastable stare (see text).

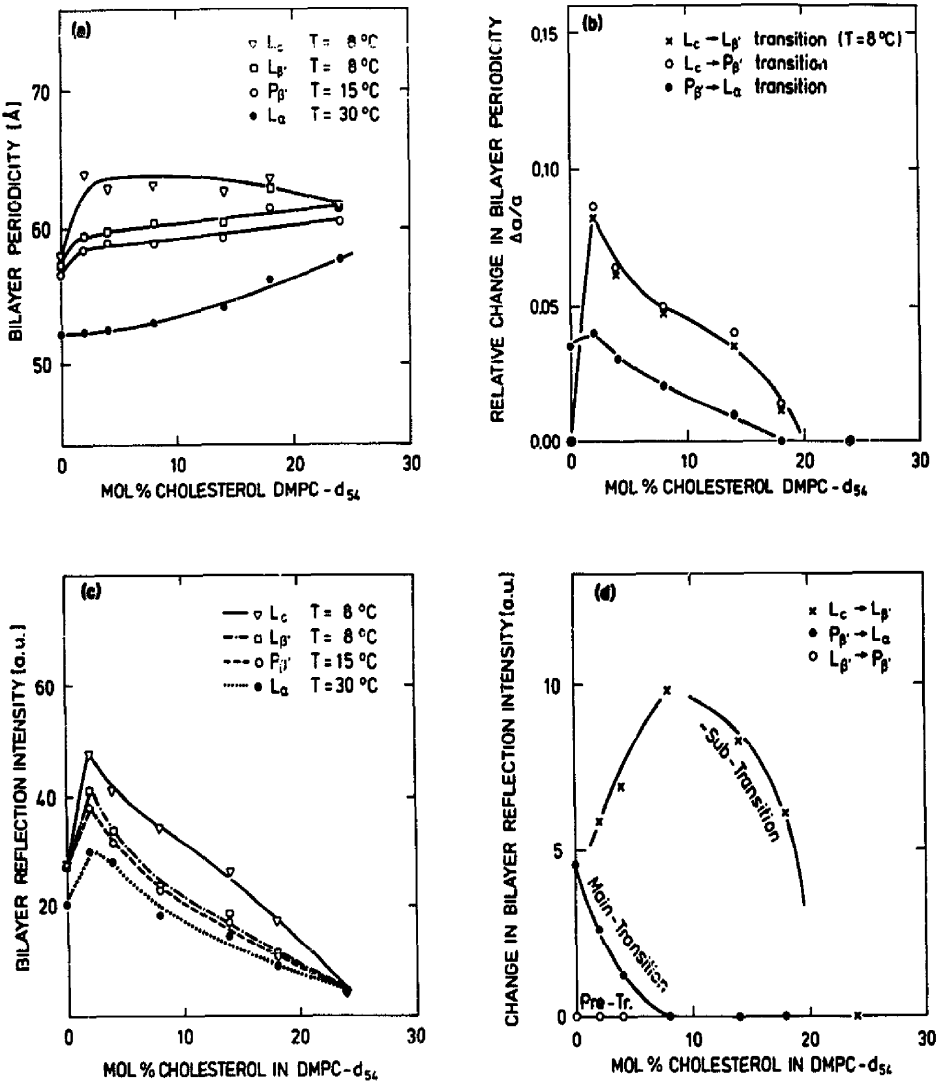

Fig. 4. Properties of the scattering peak related to the bilayer periodicity of lamellar DMPC-d_{54} plotted versus content of cholesterol, as observed in the different phases: L_c, $L_{\beta'}$, $P_{\beta'}$ and L_α. (a) Bilayer periodicity. (b) Relative change in bilayer periodicity at the various phase transitions: T_s, T_p and T_m. (c) Bilayer Bragg-peak intensity. (d) Change in the Bragg-peak intensity at the various transitions.

observed is 8% (Fig. 4a). At higher cholesterol contents, the change at T_s decreases gradually and vanish at 20 mol%, according to extrapolation. Quite similar behaviour are seen when the materials change from the metastable $L_{\beta'}$ phase to the stable sub-phase. Differences in the crystalline sub-phase of DMPC-d_{54} and $(\text{DMPC-}d_{54})_{1-x_c}$ + $(\text{cholesterol})_{x_c}$, $0 < x_c < 0.2$, are also manifested in the kinetics involved in the L_c formation. Some hysteresis observed in the pristine material during

the thermal treatment indicates time constants of the order of several hours for the L_c formation in agreement with previously published data, whereas the materials with cholesterol need months to form the sub-phase.

The intensity of the Bragg peak of the bilayer periodicity gives additional evidence of some of the phase transitions (right column of Fig. 3 and Figs .4c and 4d). Introduction of 2 mol% cholesterol causes dramatic increase in intensity in all phases (Fig. 4c), whereas further content of cholesterol causes the intensity to decrease. In the low temperature L_c phase the relationship between the intensity and the cholesterol content is near linear. The other phases might indicate some kind of change in relationship close to 8 mol%. No marked change in behaviour is observed near 20 mol% cholesterol.

In all of the bilayers with cholesterol content less than 20 mol% ($0 < x_c < 0.2$), a sub-transition is clearly observed as the scattering intensity drops markedly going from the L_c phase to the $P_{\beta'}$ phase (Figs. 3 and 4d). A maximum in this change of intensity is observed near 8 mol%. Near the main-transition a drop in intensity is observed for the compounds with cholesterol content less than 8 mol%. The 2 mol% material exhibits though in addition a marked minimum in intensity during the initial heat-treatment, whereas the successive measurements show a more regular drop near T_m. The bilayer sample with 4 mol% cholesterol shows only a drop in intensity during the initial run, but no major changes in the succeeding studies. For samples with more than 8 mol% cholesterol there is no significant changes in peak-intensity near T_m, except for eventual minor modification in the slope of the peak-intensity versus temperature. These properties point to some kind of phase boundary near 8 mol% cholesterol.

III.A.3. Discussion of the results based on bilayer periodicity

The gradual decrease in the modification of the lattice parameter at the main transition and totally absence of any changes for cholesterol content of 20 mol% and more, is in agreement with the result of Hui and He [15], who concluded that the change from the gel state to the fluid state are no longer distinctive when the cholesterol content reaches 20 mol%. This result is moreover in agreement with other physical results as for example the role of cholesterol in regulating membrane fluidity (for a recent review, see Ref. 16). Our results indicate that also the crystalline sub-phase is suppressed at cholesterol content of the order of 20 mol%.

The continuous decrease in intensity of diffraction line with increasing cholesterol content suggests that the molecular arrangement becomes increasingly disordered. For extracting maximum knowledge from this, one must of course include the changes in structure factor as due to different scattering length of cholesterol and DMPC-d_{54}. Moreover it is necessary to include assumptions on the interbilayer correlation between cholesterol positioning. This discussion goes beyond the aim of the present report.

The gradual increase of the bilayer repeat spacing observed in the liquid L_α phase may be due to stiffening of the fluid chains with increasing cholesterol content. The much stronger increase which are observed when small amounts of cholesterol are induced in the lamellar gel structures, is probably due to reduced tilt angle of the rigid acyl chains in these phases. This is in agreement with the conclusion of Hui and He [15] and with the model of Presti et al. [17]. If this interpretation is correct, then the further increase of the gel-state bilayer thickness after inducing cholesterol beyond 2 mol% might be due to further decrease in the tilt angle (see Fig. 4a, $L_{\beta'}$ and $P_{\beta'}$ phases).

In this light, however, it is difficult to explain the even stronger increase of the bilayer repeat distance in the crystalline L_c phase, which was observed when 2 mol% cholesterol was added. In the L_c phase, the acyl chains are namely supposed to be perpendicular to the membrane plane already in the pristine material [18], and changes in tilt angle can accordingly not explain increase in bilayer repetition length. One should note that the changes of the sub-phase is not 'only' a modified lattice parameter. The temperature dependence of the observed bilayer periodicity of DMPC-d_{54} is qualitatively different from that observed in the materials incorporated with cholesterol (Fig. 3). One could wonder whether the pristine material really is in the crystalline L_c phase. But our data of DMPC-d_{54} are in perfect agreement with the

previously reported crystallographic data, including the L_c sub-phase [9,18], and, moreover, the sub-phase of pure DMPC-d_{54} seems to be created on a much smaller time scale than that of DMPC-d_{54} with cholesterol, as mentioned above. It therefore seems that the sub-phase of DMPC-d_{54} with cholesterol is substantially different from that of pure DMPC-d_{54} bilayers. The relevant question is of course, where are the cholesterol molecules situated when the bilayers are in the crystalline sub-phase? The observation of major small angle scattering, which will be discussed further below, might include information on this. A possible, but probably unlikely interpretation of the scattering data is that cholesterol segregates in regions between the two amphiphilic monolayers. Alternatively cholesterol might change the hydration of the multilayers.

Independent of the nature of the changes in the changes in bilayer repetition length, the study gives valuable information on several details on the phosphatidylcholine-cholesterol phase diagram, as already emphasized. These are the value of the sub- and the main-transition temperatures versus cholesterol content; the phase boundary at very low cholesterol content ($x_c < 0.02$), which in the gel-states probably reflects modification of the hydrocarbon-chains tilt angle; and the phase boundary near 20 mol% cholesterol. Moreover there seems to be indication of changes in behaviour near 8 mol% cholesterol content. These features, which are included in the phase diagrams shown in Fig. 15, will be further discussed below.

III.B. Ripple structure

In Figs. 6–9 are shown the neutron scattering spectra, intensity versus scattering vector, for pristine DMPC-d_{54}, and DMPC-d_{54} incorporated with 2, 4, 8, and 14 mol% cholesterol, as obtained at temperatures between 5 and 30 °C. The q ranges covered are of the order of 0.007–0.070 Å^{-1}. Most of the samples did not show any changes in the scattering related to the ripple between the measurements obtained during cooling after annealing to 30 °C, and the successive heating. These are the 2, 8, 14, 18 and 24 mol% materials. The pure DMPC-d_{54}, on the other hand, showed marked changes in the scattering between the cooling and the successive heating procedure, as also observed in the investigation of the scattering pattern obtained at larger q values, discussed above. The 4 mol% material showed in addition some changes in the small angle-scattering observed between the two series of measurements, however, this did not affect the ripple structure.

Ripples are observed in bilayer blends with cholesterol content of 0, 2, 4, 8 and 14 mol%. The 18 mol% material showed no Bragg reflection, which could be associated with rippled structure, but a marked small angle scattering is probably related to distorted ripple structure with no long-range correlation. The 24 mol% material showed no evidence of ripple reflections even at q values up to 0.004 Å^{-1} (as obtained with 24 Å neutrons). Introduction of cholesterol causes marked temperature dependencies in the ripple, which may indicate substantial different physical properties involved in stabilizing the ripples of lipids with and without cholesterol.

At low temperatures, below 9–14 °C depending on composition, two well separated kind of ripple Bragg reflections are observed in materials of cholesterol content up to 4 mol%, however with marked different temperature dependence. The long wavelength ripple corresponds probably to the undulations observed previously in low-temperature freeze-fracture studies [3,4,8], and which seems to be different from the long-wavelength Λ types of ripples, which sometimes are observed in freeze-fracture studies in the $P_{\beta'}$ phase [4–7].

III.B.1. Ripple structure of DMPC-d_{54}

In Fig. 5 are shown the scattering data obtained of DMPC-d_{54} using 8 Å wavelength neutrons. The data shows the initial study (a) presumably following the phase sequence $L_c \rightarrow P_{\beta'} \rightarrow L_\alpha$, the succeeding data set obtained during cooling the sample (b) and the final set obtained during second heating (c). Fig. 10 shows the resulting peak intensity and ripple wavelength using gaussian fits to the scattering functions.

In the studies performed following the phases $L_c \rightarrow P_{\beta'} \rightarrow L_\alpha$ (the stable state), ripple structure is observed between 13.8 °C and 19.7 °C, both temperatures inclusive. The spectrum at $T = 11.8$ °C may also indicate a very weak ripple reflection, whereas the spectrum at $T = 21.8$ °C show no evidence of ripples. The ripple periodicity changes

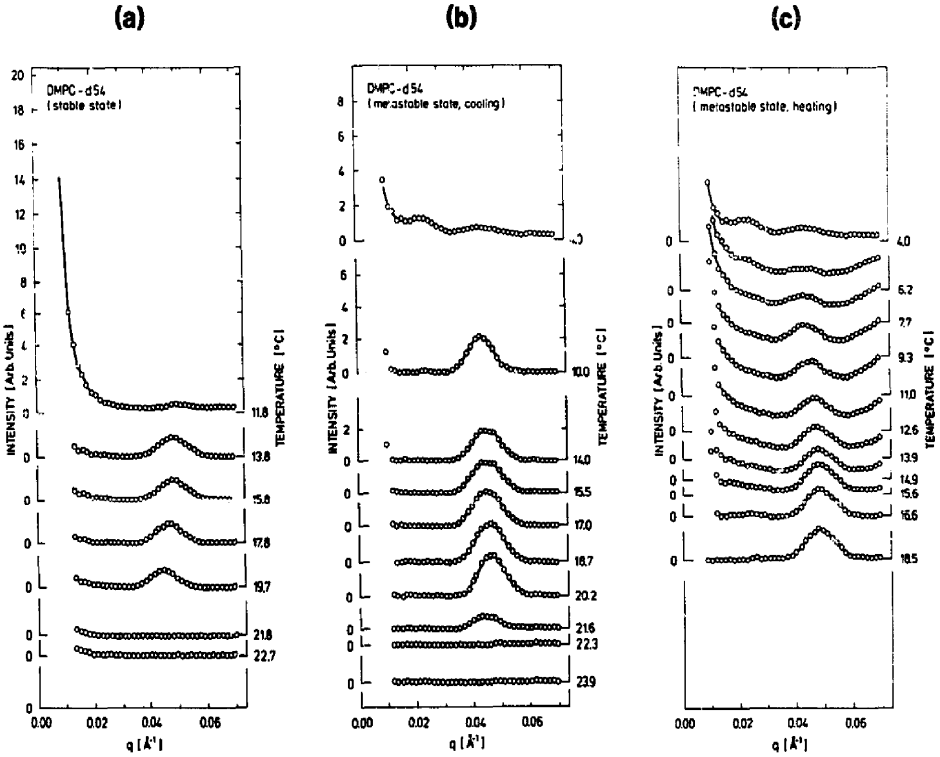

Fig. 5. Neutron scattering results, intensity versus scattering vector of DMPC-d_{54}, as obtained using 8 Å neutrons. The data show the Bragg reflection due to the ripple structure. (a) Initial set of data, following the phase sequence $L_c \rightarrow P_{\beta'} \rightarrow L_\alpha$. (b) Data obtained during cooling from 30°C, i.e. $L_\alpha \rightarrow P_{\beta'} \rightarrow L_{\beta'}$. (c) Data obtained during second heating. Note the scattering above $q = 0.06$ Å^{-1} which is the tail of low q side of the bilayer reflection, and the small-angle scattering observed at the same temperatures.

markedly within the 12–20°C regime, namely from being 123 Å at 11.8°C to be 142 Å at 19.2°C.

In the $L_{\beta'} \rightarrow P_{\beta'} \rightarrow L_\alpha$ (metastable) state, the ripple reflection intensity shows marked time dependent changes near 9°C, probably reflecting the $L_{\beta'}$–$P_{\beta'}$ pre-transition. Just below the main phase transition, the ripple wavelength shows a distinct decrease. In the low temperature metastable $L_{\beta'}$ phase, a secondary reflection appears in the scattering data, corresponding to a ripple structure with period 260 Å. The intensity of that ripple is relatively small, and vanishes at $T = 9$°C. Near the main phase transition, the primary ripple structure disappears relatively abrupt. Near the pre-transition temperature, the ripple properties seem to change more gradually, however, as the ripple structure below T_p is only slowly decaying with time, a qualitative description of the DMPC-d_{54} pre-transition is not possible on the basis of the present data sets.

III.B.2. Ripple structure of DMPC-d_{54} with 2 mol% cholesterol

Only some features of the ripple structure of DMPC-d_{54} with 2 mol% cholesterol are obviously similar to those of the pristine material. The scattering data as obtained using 8 Å and 15 Å wavelength neutrons are shown in Fig. 6, and in Fig. 10 is shown the resulting peak intensity and ripple period.

In the stable state, the rippled structure appear between $T = 16.1$ and 21.8°C, i.e. between the sub- and the main-transition. However, while the

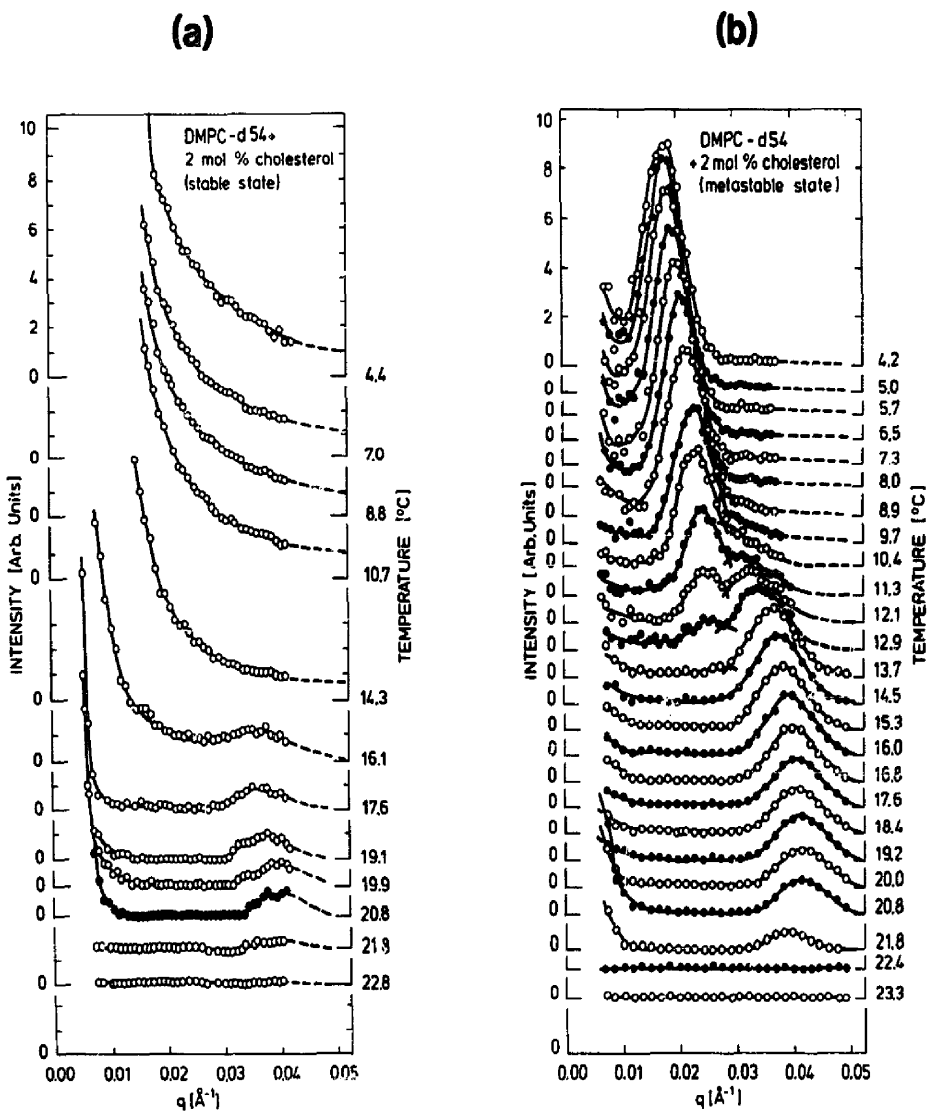

Fig. 6. Neutron scattering results, intensity versus scattering vector, of DMPC-d_{54} with 2 mol% cholesterol, as obtained using 8 Å and 15 Å neutrons. (a) Initial set of data following the phase sequence $L_c \rightarrow P_{\beta'} \rightarrow L_\alpha$. (b) Set of data following the phase sequence $L_\alpha \leftrightarrows P_{\beta'} \leftrightarrows L_{\beta'}$.

ripple periodicity of pure DMPC-d_{54} was increasing monotonously within this phase, the general tendency of the 2 mol% sample is decreasing value. The ripple wavelength varies between 170 Å and 153 Å, the minimum being below the main transition temperature, namely at 20.8°C.

In the metastable state, $L_{\beta'} \leftrightarrows P_{\beta'} \leftrightarrows L_\alpha$, the primary ripples appear between 8°C and 22°C. There was no difference in the observations obtained during cooling and during heating the sample, and there was no sign of a time dependence as that observed in pure DMPC-d_{54}. After a week at

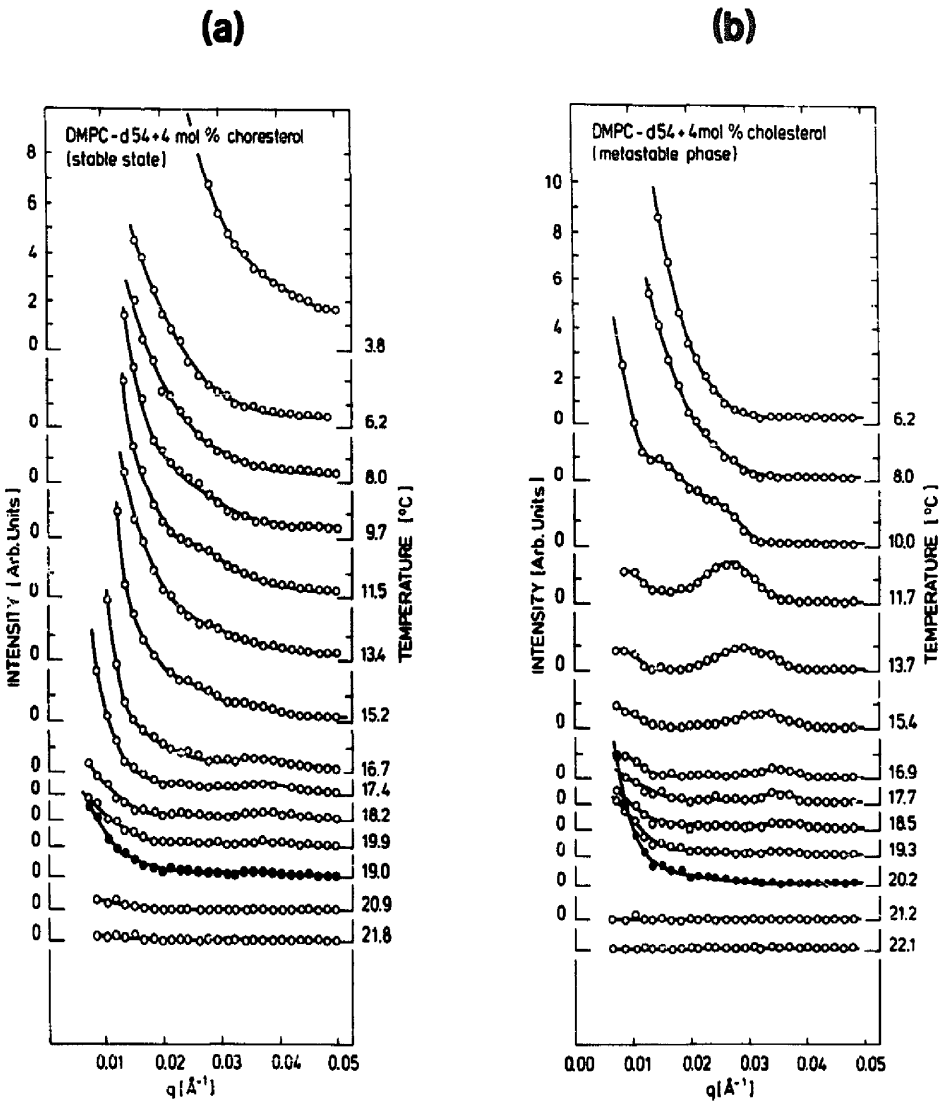

Fig. 7. Neutron scattering results, intensity versus scattering vector, of DMPC-d_{54} with 4 mol% cholesterol, as obtained using 8 Å neutrons. (a) Initial set of data following the phase sequence $L_c \rightarrow P_{\beta'} \rightarrow L_\alpha$. (b) Set of data following the phase sequence $L_\alpha \leftrightarrows P_{\beta'} \leftrightarrows L_{\beta'}$.

5 °C, there was still no sign of the stable state, which however was regained after months at this temperature. The ripple wavelength decreases very steeply near the pre-transition temperature, T_p = 9 °C, and it becomes less T-dependent at higher temperatures. Just below the main transition temperature, T_m = 22 °C, the wavelength is increasing.

The intensity of the ripple reflection shows characteristic behaviour, with an overall maximum intensity at T = 14 °C, and hint of a second maxi-

mum near 19°C, which is the maximum of the ripple structure of the stable state data.

At $T = 20°C$ there is a distinct change in the temperature dependence of the ripple peak intensity, but compared to the pure DMPC-d_{54} material, the intensity decreases more gradually.

Below the point of maximum intensity (14°C), a secondary long wavelength reflection appears in the scattering data, indicative of an other kind of ripple. A secondary low T ripple was also observed in pure DMPC-d_{54}, however, while that was rather weak, the secondary ripple of DMPC-d_{54} with 2 mol% cholesterol becomes even more intense than the primary $P_{\beta'}$ ripple. The low-temperature secondary ripple have a wavelength of 360 Å at 4°C, and it decreases to 220 Å at 14.5°C. After a week at 5°C, there was no change in the observed structure. Knoll et al. [8] reported also evidence of a secondary ripple at low temperature of a similar lipid composition.

III.B.3. Ripple structure of DMPC-d_{54} with 4 mol% cholesterol

Fig. 7 shows the scattering data of DMPC-d_{54} incorporated with 4 mol% cholesterol, and Fig. 10 includes the resulting ripple periodicity and scattering peak intensity plotted versus temperature. In the stable state, the ripple could clearly be identified between $T = 16$ and 19°C, although very weak relative to that of the other samples. Below 16°C, the scattering was dominated by small angle scattering. The ripple structure observed is similar to that observed in the metastable state at the same temperatures.

In contrast to the properties of the primary ripple of the two materials discussed above, 0 and 2 mol% cholesterol, the 4 mol% bilayer has a ripple-reflection intensity, which decreases gradually within the whole temperature regime of the metastable state, in which it is observed, i.e. 10.0–19.3°C inclusive. At 20.2°C, the ripple structure can no longer be seen, but already well below this transition temperature, the reflection is rather weak. This markedly different from the 2 mol% sample discussed above, and also from the samples of more cholesterol, which all shows tendencies of local minima in ripple amplitude well below the main transition temperature. The ripple periodicity varies monotonically between 270 Å at 10°C and 170 Å at 20°C, though with a much more steep temperature dependence at low T. Below $T = 10°C$, a different kind of scattering prevents us from observing the primary ripple.

Reversible structure in the small angle scattering curve at 10°C indicates the existence of a secondary ripple like that observed in the 2 mol% material. However, even with $\lambda = 24$ Å neutrons, we were not able to resolve the reflection, and at lower temperatures, the reflection could not be seen at all, presumably due to some kind of texture giving rise to major small angle scattering in this temperature region. The secondary ripple periodicity was estimated to be of the order of 500 Å at 10°C.

III.B.4. Ripple structure of DMPC-d_{54} with 8 mol% cholesterol

Fig. 8 shows the scattering data of DMPC-d_{54} with 8 mol% cholesterol, and in Fig. 10 is shown the derived peak intensity and the related ripple periodicity as obtained using gaussian fits. In the stable state, the ripple structure is observed between 15.0 and 19.2°C, both temperatures inclusive. In the metastable state, rippled structure is observed at all temperatures below 19.2°C. The ripple periodicity as obtained in the metastable state is 288 Å at $T = 5°C$. It decreases to a minimum of 211 Å at 16.7°C, and increases again to 233 Å at 19.2°C, which is just below the main transition temperature.

As it was observed in the study of the $x_c = 0.02$ bilayer membrane, the characteristics of the ripple studied in the stable state is also present in the data of the metastable state within the relevant temperature region.

III.B.5. Ripple structure of DMPC-d_{54} with 14 mol% cholesterol

In Fig. 9 is shown the scattering data of DMPC-d_{54} with 14 mol% cholesterol, and Fig. 10 includes the resulting data using Gaussian fits. The ripple structure shows some similarity with that of 8 mol%, although there is only a hint of the intensity minimum, which was so pronounced in the $xc = 0.08$ sample. In the stable state, rippled structure is observed between 15.7 and 18.8°C, whereas in the metastable state it is observed at all temperatures studied below 18.6°C. In the meta-

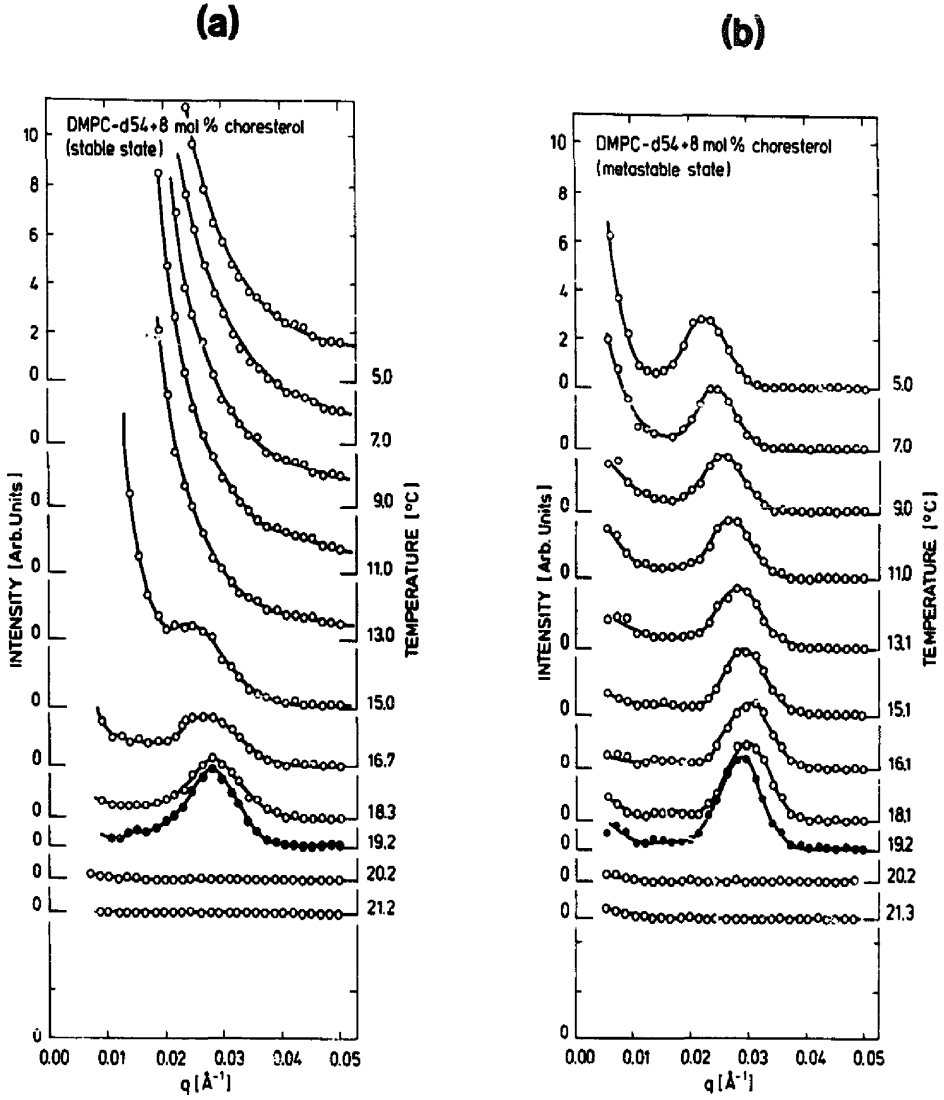

Fig. 8. Neutron scattering results, intensity versus scattering vector, of DMPC-d_{54} with 8 mol% cholesterol, as obtained using 8 Å neutrons. (a) Initial set of data following the phase sequence $L_c \rightarrow P_{\beta'} \rightarrow L_{\beta'}$. (b) Set of data following the phase sequence $L_\alpha \leftrightarrows P_{\beta'} \leftrightarrows L_{\beta'}$.

stable state there is in addition some weak, but reliably scattering up to $q = 0.04$ Å^{-1}, which may indicate minor inhomogeneities in the samples.

The ripple reflection in the stable state is pronounced weaker than that of the metastable state. While the ripple periodicity of the stable state was longer than that of the metastable state for 2 and 8 mol% cholesterol, it is markedly smaller in the 14 mol% sample. In the stable state the ripple periodicity shows moreover drastically temperature dependence, as it is 331 Å at $T = 15.7$°C and increases to 452 Å at $T = 18.8$°C. Eventual time

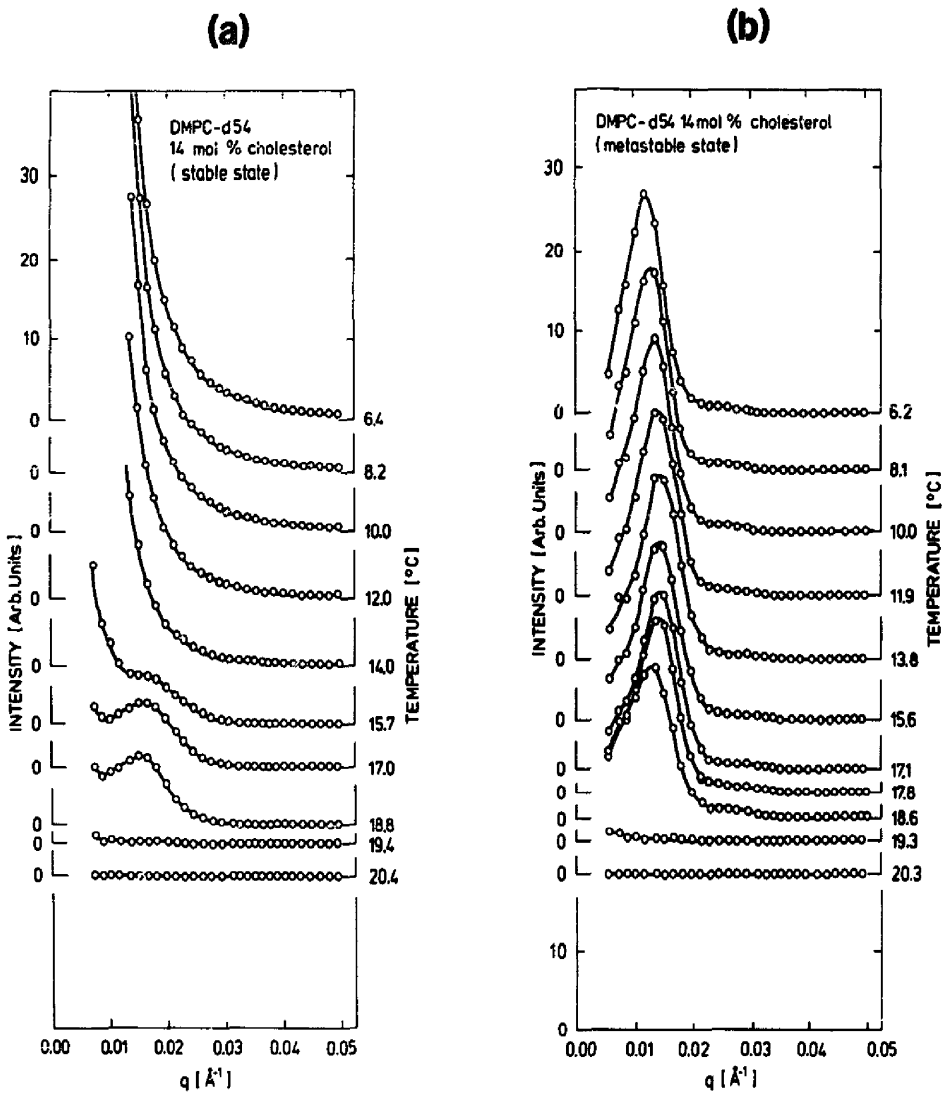

Fig. 9. Neutron scattering results, intensity versus scattering vector, of DMPC-d_{54} with 14 mol% cholesterol, as obtained using 8 Å neutrons. (a) Initial set of data following the phase sequence $L_c \rightarrow P_{\beta'} \rightarrow L_\alpha$. (b) Set of data following the phase sequence $L_\alpha \leftrightarrows P_{\beta'} \leftrightarrows L_{\beta'}$.

dependence on the ripple period in this region was not studied.

In the metastable state, the observed scattering peak intensity related to the rippled structure is very large, even larger than that of the (10)-bilayer repetition peak (see Fig. 2). The intensity decreases gradually with increasing temperature, but might give a hint of a local minimum just below the main transition, as already mentioned. The metastable ripple periodicity shows a marked minimum of 440 Å close to $T = 15\,°C$. At 6.2 °C the ripple period is 536 Å, and at $T = 18.6\,°C$,

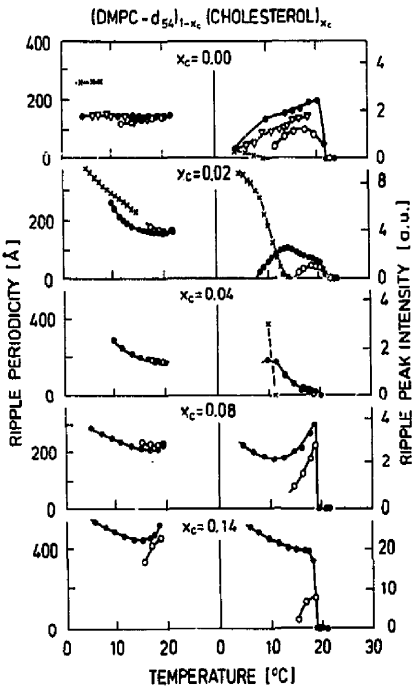

Fig. 10. Properties of the ripple structure of DMPC-d_{54} with various content of cholesterol: 0, 2, 4, 8, and 14 mol%. Open symbols represent data obtained in the stable state, whereas closed symbols and crosses are those of the metastable state (see text). The left column shows the ripple periodicity, and the right column shows the ripple Bragg-peak intensity. Note the different scales on both the plots of ripple period and of ripple peak intensity.

which is just below the main transition, the periodicity is 525 Å.

III.B.6. DMPC-d_{54} with 18 and 24 mol% cholesterol

The DMPC-d_{54} lamellar bilayers with 18 and 24 mol% cholesterol did not show any evidence of well defined rippled structure in the scattering pattern, obtained within the q-range 0.003–0.15 $Å^{-1}$ studied. But the $x_c = 0.18$ sample exhibits significant small-angle scattering below $T = 17.7°C$ which probably reflects fluctuating rippled structure, however with a regularity in wavelength, and correlation length which is too small to give rise to real Bragg peaks. This is in agreement with freeze-fracture studies, which exhibit major distortion in the ripple structure above 15 mol% cholesterol [4,6].

The $x_c = 0.24$ mixed bilayer did neither show any evidence of rippled structure nor small angle scattering, which also is in perfect agreement with freeze-fracture microscopy studies.

III.B.7. Discussion on the ripple structure of DMPC-d_{54}-cholesterol mixed membranes

In the cholesterol induced bilayer membranes, one may note that the properties of the ripple reflection observed within the stable states to a large extent also are present in the metastable data, as mentioned above, and which clearly appear from Fig. 10. If one subtracts the ripple reflection intensity observed in the stable state from that of the metastable state, one actually ends up with rather regular ripple behaviour, without the irregular I vs. T functionality directly observed. This could indicate that two different types of mechanism tend to stabilize the ripple structure. One type seems to be present only at high temperature ($T > 15°C$), and a second type seems to be most important at lower temperatures. One could argue that in the high temperature end of the metastable $P_{\beta'}$ phase, two types of domain exist, which each includes ripples of either the high temperature type or the low temperature type. But the ripple periodicity of the stable and the metastable states is clearly distinguishable, as can be seen by putting the scattering data of the metastable state on top of that of the stable state (Figs. 5–9) and which also clearly appear from Fig. 10. Therefore, it rather seems that the rippled structure gradually develops from a low temperature kind of undulation to an other kind of undulation at high temperature. It seems likely, that the high temperature ripple state is dominated by physical properties similar to those of the pristine DMPC-d_{54} bilayer membrane, i.e. the $\Lambda/2$-type of ripples according to the notation of Rüppel and Sackmann [5]. At low temperatures, on the other hand, the ripples might well be intrinsically stabilized by the cholesterol, as the cholesterol-lecithin system tends to 'phase-separate' in microscopically ordered domains. For convenience, we will here denote the proposed two kinds of undulated structure as $P_{\beta'}$ and $P_{\beta''}$ ripples for those at high and those at low temperatures, respectively.

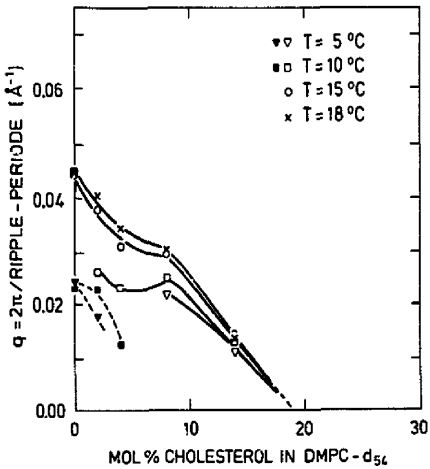

Fig. 11. Ripple periodicity as obtained from scattering experiment, plotted as 2π/periodicity versus content of cholesterol. The figure includes representative data of four different temperatures.

It is interesting to note, that the 4 mol% bilayer compound is different from that of the others, by not showing hint of a local minimum in intensity, like that observed in the other materials. From the discussion above it could seem as if the normal $P_{\beta'}$ ripple by some reason has not developed in the $x_c = 0.04$ sample, and that the ripple structure we observe up to the main transition temperature is the low T cholesterol ripple: $P_{\beta''}$. As described above, there was some problem with the $x_c = 0.04$ sample, which for example did not show any ripple reflections after storage for some more months.

As already mentioned, it has previously been anticipated that the ripple periodicity of lamellar bilayer systems is inversely proportional to the cholesterol content [4]. The present studies show, however, that this conclusion holds only for restricted temperatures as the temperature dependence of the periodicity varies differently with temperature for the various compositions (Fig. 10). In Fig. 11 is shown the inverse ripple periodicity versus content of cholesterol as determined at various temperatures. The interconnecting lines drawn between the q-values at various cholesterol content is uncertain, of course, as we in principle do not known which ripples are of the 'same physical origin' when there is more than one ripple present.

At temperatures above approximately 15 °C, i.e. when the $P_{\beta'}$ ripples are present according to the discussion above, the linear relationship between ripple periodicity and cholesterol content observed by Coleman and McConnel [4], is also observed in our studies. However, at lower temperatures, the $P_{\beta''}$ ripples show marked deviation from linearity. At cholesterol content below 8 mol%, approximately, the ripple period stays relatively constant, whereas at higher cholesterol content it follows the relationship observed at high temperature.

Several attempts have been made to explain the mechanism of forming the rippled structure of phospholipid bilayers [3,5,19–21]. The theories include a variety of models based on the packing competition between the molecular head groups and the hydrocarbon chains; elastic energy consideration leading to curved regions and precursor chain melting has been suggested as the driving force of the undulated structure. Although it presumably is of major relevance for the detailed physical understanding of the cholesterol-phospholipid interaction, in this report we will not discuss details on the mechanism behind the ripple formation in pristine lamellar structures, but restrict ourselves to a discussion on the modifications which cholesterol appears to give rise to.

In several of the models proposed, one may notice that near the peaks and/or the valleys of the zigzag structure, there is extended space available for the hydrocarbon chains. The chains are therefore probably highly distorted, and perhaps even melted in these regions. The rippled phase may thus be viewed as consisting of stripes of disordered or melted acyl chains separated by solid ordered regions. Our experimental findings clearly indicate that the cholesterol molecules in some way order regularly in the ripple structure. This is supported by the regular variation of ripple wavelength and ripple intensity with cholesterol content. On this basis we propose a model in which the cholesterol molecules (or complexes) are fixed to the distorted stripes. In Fig. 12 we show schematically the model, which is inspired by the one of Coleman and McDonnal [4]. For cholesterol content less than 8 mol% the cholesterol-com-

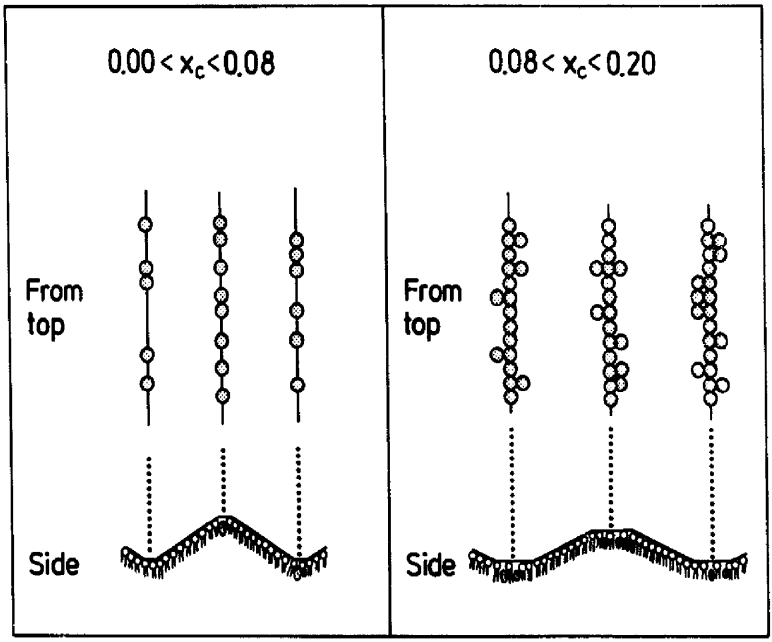

Fig. 12. Proposed model of the phosphatidylcholine-cholesterol mixed bilayer membranes in the solid gel state $P_{\beta'}$ (and $P_{\beta''}$), in which the cholesterol complexes are proposed to enter the ripple structure regularly, namely in the bottom and/or top of the zigzag structure. For cholesterol content less than 8 mol%, the impurity stripes are still not saturated with cholesterol, whereas cholesterol content above 8 mol% contains saturated, i.e. connected, stripes of complexes. Above 20 mol% cholesterol, approximately, the defect stripes overlap, and there is accordingly no ripple structure left. For simplification, we have neglected eventual asymmetry in the ripple structure.

plexes are randomly distributed within the defect lines, and the amount of cholesterol is still not large enough to form continuous domains. Macroscopic physical properties like viscosity etc. are therefore basically equal to those of the pure DMPC-lamellar material. Above 8 mol%, however, the cholesterol complexes form large connected domains (stripes) which give modified properties revealing the liquid like character of the phase of cholesterol complexes. Since the stripes in these regions are 'saturated' with cholesterol, we will index the phases with a c: $P^c_{\beta'}$ and $P^c_{\beta''}$, respectively. Above 20 mol% cholesterol, approximately, the 'defect stripes' overlap, and there is accordingly no solid ordered gel-regions left, and thereby no ripples either. The saturated cholesterol stripes observed between 8 and 20 mol% cholesterol contain according to the present model 20 mol% cholesterol. Thus each complex consists of phosphatidylcholine and cholesterol molecules in the ratio 4 : 1.

The proposed model may be viewed as phase separation on a microscopic scale. On a macroscopic scale, however, the system is isotropic also in the 8–20 mol% cholesterol regime. The model is in agreement with the neutron scattering experiments of Knoll et al. [8], in which small-angle scattering was observed between approximately 8 and 20 mol% cholesterol. In Ref. 8, however, this was interpretated as originating from an immiscibility gap, in which macroscopic domains of 8 and 20 mol% cholesterol were present. This can not be true, since that would imply unchanged ripple wavelength in the 8–20 mol% region of the phase diagram in disagreement with the marked correlation observed in the present study. Similarly, the interpretation of the model calculation by Ipsen et al. [22] may need some modifications in order to

account for the experimental observations. In Ref. 22, a thermodynamic model was proposed, in which the cholesterol molecules is assumed to induce melted phospholipids with ordered acyl chains, i.e. the model includes solid domains with ordered chains, and liquid domains, which both could have ordered and disordered chains. The thermodynamic model predicts an immiscibility gap between 8 and 20 mol% cholesterol.

The regular behaviour of the ripple versus cholesterol content observed at temperatures above $T = 15°C$, approximately, i.e. in the $P_{\beta'}$ phase according to the notation introduced above, may be understood if the physics involved in stabilizing the ripples are basically the same as that of the pristine material. The cholesterol complexes act then only as a steric perturbation of the parameters involved in stabilizing the undulated structure. It may seem somewhat surprising that the simple relationship between the $P_{\beta'}$ ripple and the cholesterol content hold even to 0 mol% cholesterol. We know namely from the study of the bilayer repetition length, which was described above, that minor content of cholesterol have dramatic influence on the bilayer periodicity. Correlated effects could be expected in the ripple structure.

At lower temperature where the $P_{\beta''}$ ripples are present, according to the discussion above, the dependence on cholesterol content is dramatically different. First of all the ripple structure is significantly stabilized by the presence of cholesterol. Moreover, we find that the undulation-period for cholesterol concentrations in the range $0 < x_c < 8$ mol% is basically constant of the order of 250 Å, i.e. about 25 phosphatidylcholine molecules (Figs. 11 and 12). For 8 mol% cholesterol, which is the concentration which appear to be some kind of phase-boundary, this corresponds to approximately two cholesterol complexes per ripple, i.e. one complex at the top and one at the bottom of the zigzag structure for example. This strongly suggests that the $P_{\beta''}$ ripples intrinsically is a result of the cholesterol complexes, which apparently form stripes of cholesterol rich domains. It is not at the moment clear, however, why the cholesterol complexes tend to make this highly ordered super-structure. For cholesterol content less than 8 mol% the impurity stripes are still not saturated chains of cholesterol complexes, as expressed in the model Fig. 12. Additional cholesterol molecules will therefore go into the stripes without modifying the periodicity significantly. For cholesterol concentrations above 8 mol%, on the other hand, there is no more room for additional complexes within a single row, and the defect strips will accordingly expand. This explains the observed change in ripple periodicity above 8 mol% cholesterol.

The simple model presented above does not explain the major temperature dependence of the ripple wavelength, which in particular was observed in the materials incorporated with cholesterol, but to a lower degree also was seen in the pure DMPC lamellar material. The raw model, as described, would on the contrary, rather predict temperature invariance, as the periodicity is given by the cholesterol-to-phospholipid ratio. One could argue for temperature dependence as due to changes in the polar-head group configuration. However, this should imply equivalent simultaneous changes in the bilayer repetition length, which is not seen. Other possible explanations could involve temperature dependencies in the tendency of creating cholesterol-complexes with various stable cholesterol-to-phosphatidylcholine ratios, as for example the 1 : 4, 1 : 6 and 1 : 7 ratios previously proposed. The picture with rows of equal cholesterol complexed may, though, very well be oversimplified. A better model should of course be made on the basis of thermodynamic interactions between the molecules involved. It could, for example, be inspired by the model of Ipsen et al. [22], in which one may include that cholesterol causes ordered acyl chains in liquid domains (stripes) of a temperature-dependent size (width). A more complete explanation should of course also include the presence of the secondary ripple structure, which was observed experimentally at low cholesterol content. This super-structure has been totally disregarded in the model presented above.

III.C. Small-angle scattering near the main transition

From Figs. 6 and 7 it is noticed, that significant small angle scattering appears in the scattering spectra near the main phase transition of the 2

and 4 mol% cholesterol samples. The scattering pattern was perfectly reproducible in coming from low and from high temperature. Corresponding small-angle scattering scattering could not be seen in any of the other mixed materials. The origin of this scattering is not known, but certainly it points to the existence of two transition temperatures in this temperature regime. The small-angle scattering is likely to originate from some kind of fluctuation in the phase composition. However, it may also be a result of other kind of texture in the bilayer system.

A splitting of the main phase transition was also observed in the thermodynamic model of Ipsen et al. in the 0–8 mol% cholesterol region of the phase diagram [22]. In that model, which, however, did not include the rippled $P_{\beta'}$ phase, the splitting was interpreted as due to coexistence of the solid ordered $L_{\beta'}$ phase and the fluid disordered L_α phase. Similarly, one might argue that the region of the phase diagram, where small angle scattering is observed experimentally, might originate from coexistence of the $P_{\beta'}$ gel state and the liquid L_α state.

III.D. Small-angle scattering of the L_c phase

The scattering patterns of the DMPC-d_{54}-cholesterol blends in the so-called stable state are dominated by major small-angle scattering below approximately 16 °C and for cholesterol contents up to and inclusive 18 mol%. The temperature at which the small-angle scattering vanishes depends only slightly on the cholesterol content. We believe that the small-angle scattering reflects properties of the crystalline L_c phase, and that the suppression of the scattering is related to the sub-transition.

The small-angle scattering pattern shows no sign of any characteristic length scale of the properties giving rise to it. On the contrary, the scattering curves are basically linear in the double logarithm plot: $\log(I)$ versus $\log(q)$, and with a non-integer value of the index of slope. Thus the samples are characterized as being selfsimilar within the sizes determined from the q values (60 Å $< \pi/q <$ 600 Å), with a fractal dimension which for all materials in discussion, except maybe the 0 and 2 mol% samples, are between 2.8 and 3.0.

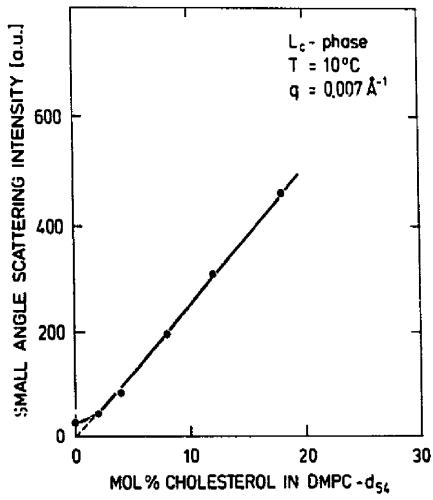

Fig. 13. Intensity of the small angle scattering intensity of $(\text{DMPC-}d_{54})_{1-x_c}+(\text{cholesterol})_{x_c}$ versus content of cholesterol, x_c. The scattering intensity is represented by the values observed at $q = 0.007$ Å^{-1}.

The origin of the small-angle scattering is presently not known. Although the pristine material also shows some small angle scattering in the low temperature crystalline state, there appears to be a simple relationship between the measured absolute small-angle scattering intensity and the cholesterol content (Fig. 13), thus indicating that the scattering is mainly caused by the cholesterol. As there seem to be no ripples or stripes in the texture of the L_c phase, the cholesterol (or cholesterol complex) is not lined up as discussed in relation to the $P_{\beta'}$ phase. In the dense crystalline packing of the L_c phase, it seems likely that the cholesterol molecules will not enter the bilayer randomly, but rather phase-separate into cholesterol-rich domains. We propose that it is the structure of these domains which gives rise the fractal small-angle scattering. An alternative explanation of the scattering may be texture in the crystalline material. In freeze-fracture studies Singer and Finegold [2] have observed crinkled surface profiles in other phospholipid bilayers when stored for long times at low temperatures. Such profiles would also give rise to small-angle scattering, however, it would not explain the regular dependence on cholesterol content. Moreover,

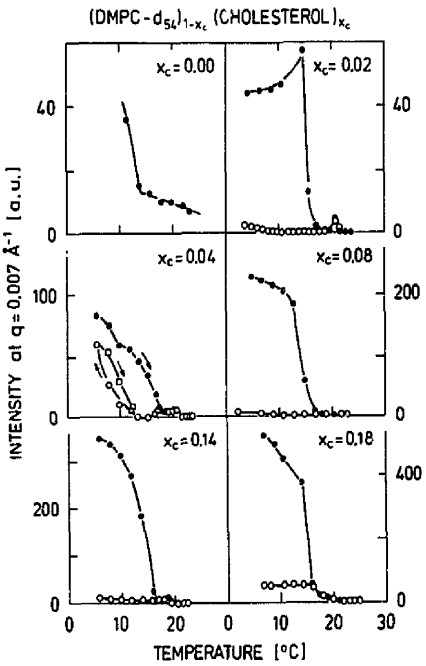

Fig. 14. Small-angle neutron scattering intensity, as represented by the values obtained at $q = 0.007$ Å^{-1}, plotted versus temperature for various composition of DMPC-d_{54} and cholesterol. The closed symbols represent data obtained in the stable state, whereas the open symbols are those of the metastable state.

and to some extent in agreement with our small-angle studies, Singer and Finegold did not observe the circled texture in DMPC-samples, and they discussed whether the texture eventually was an artificial result of the freeze-fracture technique when used on the rigid crystalline L_c phase.

The small-angle scattering disappears rather abruptly at a transition temperature which we relate to the $L_c \rightarrow P_{\beta'}$ sub-transition. However, as the scattering curves are linear in a log-log plot, it is not possible to obtain any extrapolated zero-angle intensity. In Fig. 14 we have therefore plotted the intensity at an arbitrary low q value, namely $q = 0.007$ Å^{-1}, as a function of temperature. The sub-transition is easily extracted from these figures.

IV. Phase diagram of DMPC-d_{54}-cholesterol system

It appears from the previous sections, that many details on the phosphatidylcholine-cholesterol phase diagram can be extracted from the structural data already discussed.

The $L_c \rightarrow P_{\beta'}$ sub-transition temperature can be obtained first of all from the small-angle scattering of the L_c-phase, Fig. 14. But also the bilayer periodicity and the intensity of the corresponding neutron scattering Bragg reflection give clear evidence of the transition temperature. The main $P_{\beta'} \leftrightarrows L_\alpha$ transition temperature can also be obtained from structural features of the bilayer periodicity, as well as from the upper temperature at which the ripples disappear. However, significant small-angle scattering of the 2 and 4 mol% samples at temperatures near the main phase transition clearly show that there is no direct phase-boundary between $P_{\beta'}$ and L_α of these cholesterol content. Apparently, addition of cholesterol leads to a splitting of the $P_{\beta'} \rightarrow L_\alpha$ transition into liquidus and solidus line, and thereby probably to the coexistence of the two phases in the two phases in a small temperature region.

The $L_{\beta'} \leftrightarrows P_{\beta'}$ (or $P_{\beta''}$) pre-transition can be observed only from the ripple structure, which vanish below T_p. The bilayer periodicity, except for that of the pristine DMPC-d_{54} material, shows no significant change at the pre-transition.

Additional information of the phosphatidylcholine-cholesterol phase-diagram are obtained from the ripple structure, as already discussed above. The change in dependence of cholesterol at $x_c = 0.08$ suggests a phase boundary at this point, namely toward saturated stripes of cholesterol-complexes for $x_c > 0.08$, as discussed above. Both the properties of the bilayer and the ripple periodicities point in addition to a second phase boundary at cholesterol content of the order of 20 mol% (Fig. 4b and Fig. 11).

Additional changes are seen in the structural properties of DMPC-d_{54} cholesterol blends, which can not be related to the well known transitions, sub, pre and main. This is the indication of different kind of rippled structure at low and at high temperatures of the $P_{\beta'}$ phase, thus indicating two rippled phases: the $P_{\beta'}$ phase analog to that of

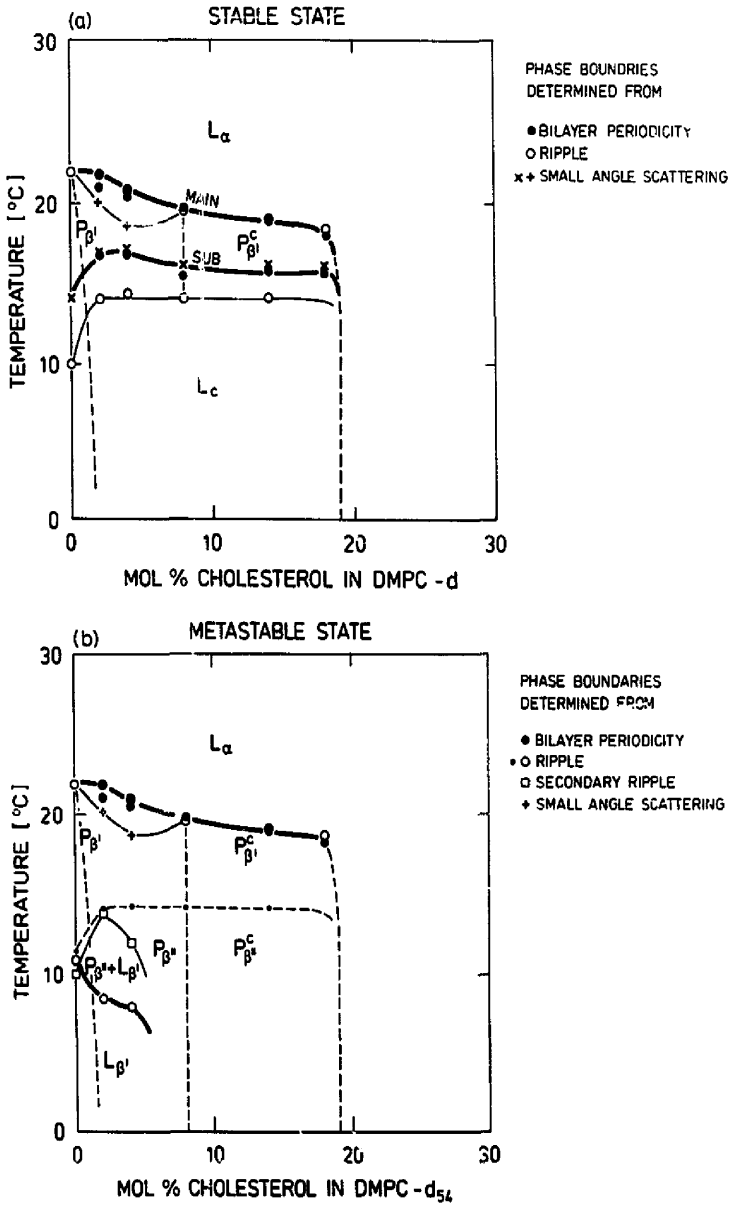

Fig. 15. Phase diagram of DMPC-d_{54} cholesterol mixture, as obtained from the structural information on bilayer periodicity, rippled structure and small angle scattering. Figure (a) represents the diagram observed after storage at 5 °C for months (stable state), while figure (b) is the diagram observed just after preparation, and after annealing at 30 °C (metastable state).

pure DMPC-d_{54} and a cholesterol induced $P_{\beta''}$ phase as suggested above. Moreover there is the appearance of a secondary long wavelength ripple structure at low temperatures of the composition of low or non cholesterol content.

In Fig. 15 we have summarized the experimen-

tal evidences of phase transitions within two phase-diagrams of DMPC-d_{54} cholesterol blend, namely that observed while heating after storage at 5°C for months, and that observed just after preparation or equally well after storage and annealing in the fluid L_α phase (30°C). The feature that the sub-transition is above the pre-transition ($T_p < T_s$) complicates the phase-diagram somewhat, and makes it most suitable presented in two figures, as done. The phase diagram agrees with that previously reported for DMPC (and DPPC)/cholesterol mixtures [11,13,22], which, however, only include properties near the main phase-transition, and which in addition shows behaviour in the fluid phase which could not be detected with our technique.

At the present, the relevant interactions parameters involved in the formation of the observed phase diagram is not known. Initial attempts to make a thermodynamic model has, as already mentioned above, recently been proposed by Ipsen et al. [22]. Some features on the bilayers are, however, disregarded in that model. This is especially the rippled $P_{\beta'}$ phase, which we believe is of major importance for the full understanding of the phosphatidylcholine-cholesterol phase diagram. In the model proposed in Ref. 22 three states are included: (i) A solid phase with conformational ordered hydrocarbon chains (so) corresponds to the $L_{\beta'}$ gel phase, (ii) a liquid phase with conformational disordered hydrocarbon chains (ld) corresponds to the L_α phase, and finally (iii) there is a cholesterol rich ($x_c > 20$ mol%) liquid state with conformational ordered chains (lo). The model calculation based on these states gives agreement with several known properties, as for example the immiscibility gap suggested on the basis of small-angle neutron scattering. However, as mentioned above, our data certainly show that the immiscibility is not on a macroscopic scale. That would namely imply that the basic properties of the ripple structure was the same for the 8 mol% and the 14 and 18 mol% samples, which is certainly not the case. On the contrary, there is a marked change in ripple periodicity also in the 8–20% regime of the phase diagram. As discussed above, this rather points to a regular 'phase separation' on a microscopic scale, only, namely with the cholesterol complexes lined up in the ripple stripes. Above 8 mol% cholesterol, we suggests that the stripes are saturated with cholesterol, i.e. the ripples may in this phase-region be viewed as composed of lo-stripes separated by so-regions, according to the language of Ref. 22.

The model-calculation of Ipsen et al., results moreover in a two-phase region in the all liquid phase, namely consisting of one phase with liquid-ordered and one phase with liquid-disordered chains. This finding is supported by data of calorimetric and magnetic resonance techniques. Our study does not, however, show any indications of such an immiscibility gap at high temperature. The present scattering study can, of course, not reject the existence of such a gap, but we would expect major small angle scattering at least near the phase boundaries, where composition fluctuations should be present.

V. Conclusions

In conclusion we have shown that neutron scattering experiments on (DMPC-d_{54})$_{1-x_c}$ + (cholesterol)x_c obtained at small angles give detailed insight in the phosphatidylcholine-cholesterol phase diagram, and in the effect of cholesterol on the ripple structure. Cholesterol is seen to have a substantial stabilizing effect on the fluid L_α phase, which above 20 mol% is present to the lowest temperatures studied (5°C). At lower cholesterol content, the introduction of cholesterol in the amphiphilic bilayer planes moreover stabilize the rippled structure. Ripples are observed for cholesterol content up to 14 mol%, and small-angle scattering suggest further disordered ripples up to approx. 20 mol%. Major temperature dependencies are observed in the ripple periodicity of the cholesterol induced samples, and up to approx. 4 mol%, a secondary ripple is observed at low temperatures. The data indicates that cholesterol order regularly in respect to the ripple structure. We suggest that the complexes are fixed in the defect lines established by the bottom and/or top of the zigzag structure. Above 8 mol% cholesterol content, the cholesterol complexes form continuous liquid-like stripes, which explain the observed change in fluidity at this ratio. At 20 mol% the impurity stripes make up the whole membrane, and there is accordingly no ripples left. The low-

temperature stable sub-phase is created only after months below the sub-transition temperature. It seems that the highly crystalline (L_c) sub-phase of the pristine DMPC-d_{54} material is substantially different from the sub-phase of samples with cholesterol. Marked small-angle scattering, which is observed in the latter phases, indicates that cholesterol aggregates in special, eventual fractal, structures.

Acknowledgements

Illuminating discussions with T. Henckel, O.G. Mouritsen, J.H. Ipsen and M.J. Zuckermann are gratefully acknowledged. The Risø Small-Angle Neutron Scattering facility was established by the support from the Danish and the Swedish natural science research councils.

References

1 Tardieu, A., Luzatti, V. and Reman, F.C. (1973) J. Mol. Biol. 75, 711–733.
2 Janiak, M.J., Small, D.M. and Shipley, G.G. (1976) Biochemistry 15, 4575–4580; (1979) J. Biol. Chem. 254, 6068–6078.
3 Sackmann, E., Rüppel, D. and Gebhardt, C. (1980) Springer Series in Chem. Phys. 2, 309–326.
4 Copeland, B.R. and McConnel, H.M. (1980) Biochim. Biophys. Acta 599, 95–109.
5 Rüppel, D. and Sackmann, E. (1983) J. Phys. 44, 1025–1034.
6 Hicks, A., Dinda, M. and Singer, M.A. (1987) Biochim. Biophys. Acta 903, 177–185.
7 Zasadazinski, J.A.N. and Schneider, M.B. (1987) J. Phys. 48, 2001–2011.
8 Knoll, W., Schmidt, G., Ibel, K. and Sackmann, E. (1985) Biochemistry 24, 5240–5246.
9 Mattai, J., Sripada, P.K. and Shipley, G.G. (1987) Biochemistry 26, 3287–3297.
10 Singer, M.A. and Finegold, L. (1985) Biochim. Biophys. Acta 816, 303–312.
11 Mabrey, S., Mateo, P.L. and Sturtevant, J.M. (1978) Biochemistry 17, 2464–2468.
12 Knoll, W., Haas, J., Stuhrmann, H.B., Fuldner, H.H., Vogel, H. and Sackmann, E. (1981) J. Appl. Cryst. 14, 191–202.
13 Recktenwald, D.J. and McConnel, H.M. (1981) Biochemistry 20, 4505–4510.
14 Sackmann, E. (1983) Biophysics (Hoppe, W. et al., eds.), pp. 425–457, Springer Verlag, Heidelberg.
15 Hui, S.W. and He, N.-B. (1983) Biochemistry 22, 1159–1164.
16 Presti, F.T. (1985) Membr. Fluidity Biol. 4, 97–146.
17 Presti, F.T., Pace, R.J. and Chan, S.I. (1982) Biochemistry 21, 3831–3835.
18 Ruocco, M.J. and Shipley, G.G. (1982) Biochim. Biophys. Acta 684, 59–66; 691, 309–320.
19 K. Larsson, K. (1977) Chem. Phys. Lipids 20, 225–228.
20 Georgallas, A. and Zuckermann, M.J. (1986) Eur. Biophys. J. 14, 53–61.
21 Carlson, J.M. and Sethna, J.P. (1987) Phys. Rev. A36, 3359–3374.
22 Ipsen, J.H., Karlstrom, G., Mouritsen, O.G., Wennerstrom, H. and Zuckermann, M.J. (1987) Biochim. Biophys. Acta 905, 162–172.